Laser Surface Alloying of Aluminium with WC+Co+NiCr for Improved Wear Resistance

Subhasisa Nath, Sisa Pityana, Jyotsna Dutta Majumdar

PII: S0257-8972(12)00054-0
DOI: doi: 10.1016/j.surfcoat.2012.01.038
Reference: SCT 17298

To appear in: *Surface & Coatings Technology*

Received date: 28 September 2011
Accepted date: 19 January 2012

Please cite this article as: Subhasisa Nath, Sisa Pityana, Jyotsna Dutta Majumdar, Laser Surface Alloying of Aluminium with WC+Co+NiCr for Improved Wear Resistance, *Surface & Coatings Technology* (2012), doi: 10.1016/j.surfcoat.2012.01.038

Laser Surface Alloying of Aluminium with WC+Co+NiCr for Improved Wear Resistance

Subhasisa Nath[1], Sisa Pityana[2] and Jyotsna Dutta Majumdar[1*]

[1]Department of Metallurgical & Materials Engineering, IIT Kharagpur, West Bengal, India
[2]National Laser Centre, CSIR, Pretoria, South Africa

Abstract

In the present study, laser surface alloying of aluminium with WC+Co+NiCr (in the ratio of 70:15:15) has been conducted using a 5 kW continuous wave (CW) Nd:YAG laser (at a beam diameter of 0.003 m), with the output power ranging from 3-3.5 kW and scan speed from 0.012 m/s to 0.04 m/s by simultaneous feeding of precursor powder (at a flow rate of 1×10^{-5} kg/s) and using He shroud at a gas flow rate of 3×10^{-6} m^3/s. The effect of laser power and scan speed on the characteristics (microstructures, phases and composition) and properties (wear and corrosion resistance) of the surface alloyed layer have been investigated in details. Laser surface alloying leads to development of fine grained aluminium with the dispersion of WC, W_2C, Al_4C_3, Al_9Co_2, Al_3Ni, $Cr_{23}C_6$, and Co_6W_6C. The microhardness of the alloyed zone is significantly improved to a maximum value of 650 VHN as compared to 22 VHN of the as-received aluminium substrate. The mechanism of microhardness enhancement has been established. The fretting wear behavior of the alloyed zone was evaluated against WC by Ball-on-disc wear testing unit and the mechanism of wear was established.

Keywords: Laser surface alloying; aluminium; WC; microstructure; microhardness; wear

*corresponding author, FAX.: +91 3222 282280, e-mail: jyotsna@metal.iitkgp.ernet.in

1. Introduction

Aluminium and its alloys have potential state of application in aerospace and automotive industries because of low cost, light weight and good strength [1]. However, poor wear resistance of these alloys causes problem on wide scale application of their alloys [1]. As wear is a surface dependent engineering properties it may be improved by the modification of microstructure and composition of near surface region of the component [2]. Laser surface alloying is an emerging route of modifying the microstructure and composition of the near surface region of a component by melting the surface using a high power laser and simultaneous addition of alloying constituents in the molten pool [3]. Laser surface alloying may also be used for dispersion of ceramic materials into metallic matrix and hence, form a ceramic dispersed metal matrix composite on metallic substrate [3]. The advantages of laser surface alloying include refinement of the microstructure, uniform dispersion of ceramic particles with minimum interfacial dissolution, a good bonding with the substrate and a narrow heat affected zone [3]. However, laser parameters should be properly chosen to ensure a defect free and homogeneous microstructure. The process has also been successfully applied for development of SiC, Al_2O_3, Cr_2C_3 dispersed magnesium matrix composite in magnesium and SiC dispersion iron matrix composite on mild steel [4-6]. In the past, attempts have also been made to enhance the wear resistance of aluminum by surface alloying with Ni, Fe, Cu, Mo and Cr [7-13]. Attempts have also been made to improve wear resistance of aluminium by laser composite surfacing with silicon carbide and titanium carbide [14,15]. In all the cases, a significant improvement in wear resistance properties was noticed.

In the present study, development of tungsten carbide (WC) disperse surface has been attempted on aluminium matrix by laser surface melting and simultaneous deposition of WC+Co+NiCr (in the ratio of 70:15:15) in the molten aluminium. Co and NiCr have been added as a binder to increase the wettability of WC in aluminium matrix [16]. In this regard, it

is relevant to mention that dissociation of carbides during laser processing promotes alloy carbide formation and its depletion in the matrix, which causes deterioration of corrosion resistance property of the substrate. Furthermore, presence of carbide in the matrix also increases the probability of galvanic corrosion in the substrate [17]. Hence, NiCr have been added as a binder to compensate for the deterioration of corrosion resistance property. A detail study was undertaken to investigate the effect of laser parameters on the microstructure, phases and composition of the composite layer and detail study of effect of composite surfacing on microhardness and its variation.

2. Experimental

In the present study, commercially pure aluminium samples of dimension: 0.02 m x 0.02 m x 0.005 m were sand blasted (using Al_2O_3 particles of 10-25 μm particle size) and subjected to laser surface alloying using a 5 kW fiber optics delivery Rofin-Sinar Nd:YAG (Model: KUKA KR60L30HA) laser operating in continuous wave (CW) mode (at a beam diameter of 0.003 m) by simultaneous feeding of 70WC-15Co-15NiCr (prepared by mixing the elemental powders in the said weight ratio using a high energy ball mill at a speed of 31 rad/s for 2700 s) of average particle size in the range of 25 μm to 60 μm (in the ratio of 70:15:15) in the molten pool and using He as shrouding environment (at a flow rate of 3×10^{-6} m^3/s). A large number of trials were undertaken under a wide range of laser power and scan speed combinations to optimise the laser parameters for laser surface alloying operation. The optimum laser parameters used in the present study were as follows: applied power from 3 to 3.5 kW, scan speed ranging from 0.012 to 0.04 m/s and powder feed rate of 1×10^{-5} kg/s. Selection of laser parameters outside the chosen optimum range lead to either inadequate melting or formation of defects in the microstructure of the alloyed zone. In the present experiment the weight ratio of powders was selected based on optimum quality of the alloyed

zone in terms of uniform microstructure, hardness and toughness of the alloyed zone and supported by literatures study. Figure 1(a) shows the scanning electron micrograph of the premixed precursor powders used in the present study. From Figure 1(a), it is evident that the all particles used in the present study are irregular in shape. Furthermore, Co, Ni and Cr particles are significantly refined due to repeated interaction with hard WC particles and hard balls during ball milling operation. Figure 1(b) shows the X-ray diffraction profile of the precursor powder which evidences the presence of WC, Co, Ni and Cr in the precursor powder. A relatively low intensity of Co, Ni and Cr in the X-ray diffraction profile is attributed to a low mass fraction of the respective powders in the precursor powder mixture. Followed by laser surface alloying, the microstructures of the coating (both the top surface and the cross section) were characterized by field emission scanning electron microscopy (SUPRA 40, Zeiss SMT AG, Germany) and high resolution transmission electron microscopy (JEM – 2100, JEOL, Japan). A detailed analysis of the phase and composition was carried out by X-ray diffraction technique (D8 Advances, Bruker AXS, Germany), electron back scattered diffraction (EBSD) (Oxford Channel-5 EBSD Detector) technique and energy dispersive X-ray spectroscopy (EDS) (OXFORD INCA EDS detector), respectively. The microhardness of the coated surface (both on the top surface and along the cross sectional plane) was measured by a Vickers microhardness tester (UHL-VMHT, Leica) using a 0.025 kg applied load. The kinetics of wear was evaluated using fretting wear tester (DUCOM, TR-283M-M4) against WC ball (hardness 2242 VHN, data from supplier) of 0.006 m diameter. The wear tests were carried out with varying normal load (0.5 kg, 1 kg) for constant testing duration (1800 s) at constant frequency (10 s^{-1}) and constant stroke length 0.001 m. With the help of Winducom 2006 software the cumulating loss of depth with time was calculated.

3. Results & Discussions

3.1 Microstructural Characteristics

Figures 2(a,b) show the scanning electron micrographs of cross-section of laser composite surfaced aluminium with WC+Co+NiCr lased with a laser power of 3.5 kW and scan speed of (a) 0.04 m/s and (b) 0.012 m/s. From Figure 2, it may be noted that microstructure is composed of dispersion of carbides in aluminium matrix. The depth of alloying and the area fraction of the dispersants were found to vary with processing parameters. A detailed study shows that increase in applied power and decrease in scan speed (within the applied process parameters in the present study) increases the depth of alloyed zone and vice-versa. The increase in depth of alloyed zone with increase in applied power or decrease in scan speed is attributed to an increase energy density available. Comparison between Figure 2(a) and Figure 2(b) shows that application of high scan speed leads to uniform dispersion of the ceramic particles in the melt zone which is attributed to melting, rapid intermixing and solidification due to a very low laser-matter interaction time. Furthermore, the alloyed zone was free from any defects like micro-porosities or cracks. Furthermore, the average surface roughness was increased from 7.5 μm to 15 μm when the scan speed of laser was decreased from 0.04 to 0.012 m/s. The increased surface roughness at a lower scan speed is attributed to increased energy density (= power density x beam diameter/scan speed) delivered due to an increased interaction time and hence, surface evaporation effect leading to roughening of surface. Decrease in scan speed caused a marginally higher mass fraction of total carbide content in the alloyed zone. However, there was an increased dissolution of WC while laser melting operation and hence, causing a more mass fraction of W_2C and other secondary carbides in the alloyed zone. As a result the overall carbide content in the alloyed zone was also increased due to decrease in scan speed. Increased area fraction of carbides at low scan speed is due to a larger quantity of alloying additions in the molten zone because of a high interaction time (due to decrease in scan speed) and hence, increase in density of the melt

zone. A detailed study of the variation of depth of the alloyed zone with laser parameters shows that with increase in applied power, initially the depth of alloyed zone increases but decreases at a very high power level. Initial increase in alloyed zone depth with applied power is attributed to an increased energy absorbed on the surface due to application of high power. At a very high power, there is decrease in the depth of alloyed zone due to evaporation of materials from the surface. On the other hand, increase in scan speed initially increases the depth of melting following which it decreases. Initial increase in depth of melting with increase in scan speed is attributed to a lower amount of particles incorporated in the melt zone with increase in scan speed leading to more power available for melting. In the other hand at a very high scan speed, the depth of the melt zone significantly decreases due to availability of very low energy input for melting operation.

A detail study of the microstructure of the top surface and cross-section was investigated to understand the effect of particle dispersion of the microstructure on the composite layer. Figures 3(a,b) show the scanning electron micrographs of the top surface (in as lased condition without polishing) formed in laser surface alloyed aluminium with 70WC+15Co+15NiCr lased with a power of (a) 3.00 kW, (b) 3.5 kW and scan speed of 0.012 m/s. From Figure 3(a), it is evident that the top surface microstructure is defect free and continuous. The dimension of individual track is 800 µm with overlap of 200 µm in both sides. Furthermore, the uniform track width from one corner to other evidences that there is no deflection of laser beam. Presence of micro-pores was also observed on the surface with the presence of few unmelted particles on the surface causing formation of rough surface. The defect content on the surface (microcracks, surface crater and roughness) was however, found to increase under unfavourable lasing conditions (applied power of more than 3.5 kW with a scan speed of less than 0.01 m/s and a power of less than 3 kW with scan speed of more than 0.04 m/s). Figure 3(b) shows the presence of large micro-cracks generated predominantly due

to a large quench stress developed during cooling. Furthermore, there is also formation of surface crater leading to increasing surface roughness when an excessive laser power or a very low scan speed is applied for lasing.

Figures 4(a-d) show the scanning electron micrographs of (b) top surface (zone 1), (c) intermediate zone (zone 2) and (d) near interface zone (zone 3) of (a) laser surfaced alloyed of aluminium lased with a power of 3 kW and scan speed of 0.012 m/s. From Figures 4(b,d), it is clear that the microstructure of the alloyed zone consists of presence of carbides in agglomerated spherical form and acicular morphology dispersed in grain refined aluminium alloy. A close comparison of Figures 4(b,c) with Figure 4(d) also reveals that the area fraction of agglomerated precipitates is much lower as compared to that of acicular shaped carbides. The microstructure of the precipitates at high magnification (cf. Figure 5) reveals that the precipitates are in the form of agglomerated globules, faceted and acicular. A detail composition analysis by energy dispersive spectroscopic study was undertaken to recognize the nature of precipitates. Table I summarizes the composition of the individual precipitates as marked in Figure 5. From Table I, it may be noted that the globular precipitates are predominantly WC. Zone 2 and 3 are WC rich and mixture of WC +Al_4C_3. On the other hand, zone 4 is predominantly Al rich with the presence of minor precipitates of other elements. The variation of size of the globular WC particles is due to partial dissolution of the particles during/before laser processing operation. The partially dissolved WC leads to formation of carbides of chromium and aluminium (as confirmed by X-ray diffraction analysis) followed by intermixing with matrix. The size of the globular precipitates were however varied at different regions and varied with laser parameters. A close look of the WC particle shows that they are indeed agglomeration of fragmented WC (Figure 6). The fragmentation of WC particles is attributed to excessive heating of the particles due to laser assisted heating and a rapid quenching and subsequently, it's entrapment within the molten aluminium. A detailed

study of the WC matrix interface (cf. Figure 6) shows that the interface is adherent and defect free. Figure 7 shows the scanning electron micrograph of the solid-liquid interface which evidences that it is defect free and continuous in nature. Furthermore, the microstructure is columnar in morphology with a large degree of refinement growing from the solid-liquid interface with a minimum area fraction of precipitates. The morphology of the microstructure changes from columnar to dendritic with a large interdendritic spacing towards the middle of the alloyed zone. The large degree of refinement at the near interface region is attributed to a large cooling rate associated with self quenching effect associated with the presence of metallic substrate.

Figures 8(a,b) show the high resolution transmission electron micrographs of laser surface alloyed aluminium showing (a) matrix and (b) precipitates. The matrix phase consists of aluminium with the signature of its partial amorphization (as evident from the SAD pattern). The partial amorphization of the matrix was achieved due to the supersaturation of the alloying elements in the matrix. Figure 8(b) confirms the dissolution of WC particle at the particle matrix interface. The SAD of the interface confirms the presence of W_2C phase due to dissolution of WC particles. A close look at the interface between the WC particle and matrix shows that the interface is defect free and continuous. The presence of dislocations were also observed at the interface which is attributed to presence of large stress attributed to the difference in coefficient of thermal expansion coefficient and a large cooling rate associated with laser processing.

3.2 Phase & Composition Analysis

A detailed study of X-ray diffraction profile of the composite layer was undertaken to understand the effect of laser surface alloying on the phases formed on the surface. Furthermore, an extensive effort was undertaken to observe the effect of process parameters on the phases formed and its quantification. Figure 9(a) shows the XRD profiles of the top

surface of laser surface alloyed aluminium with WC+Co+NiCr (at a ratio of 70:15:15) lased with a power of 3 kW and 3.5 kW at a scan speed of 0.012 m/s. Figure 9(b) shows the XRD profiles of the top surface of laser surface alloyed aluminium with WC+Co+NiCr (at a ratio of 70:15:15) lased with a power of 3.5 kW at a scan speed of 0.012 m/s, 0.03 m/s and 0.04 m/s, respectively. From Figure 9, it is clear that microstructure of the composite layer is composed of a numbers of carbides like W_2C, WC, Al_4C_3, Co_6W_6C, $Cr_{23}C_6$, intermetallics of Al and Ni (Al_3Ni), intermetallics of Al and Co (Al_9Co_2) and Al. The main phases formed due to laser surface alloying were predominantly WC, W_2C, Al_4C_3 and Al. From Figure 9, it is also evident that there is partial amorphization of the alloyed zone attributed to a large supercooling associated with rapid solidification in laser surface alloying operation. A close comparison between Figure 9(a) with Figure 9(b) shows that there is no significant difference in phase formation due to change in applied power. However, a marginal difference in peak intensity and peak broadening was observed due to change in applied power. A detailed quantitative analysis of the individual phase was calculated by RIR technique from the peak intensity [18]. On the other hand, the lattice strain developed in the matrix was calculated from the peak broadening by the application of Shrerrers formula [18]. Table II summarizes the phases formed, relative mass fraction of WC, W_2C, Al_4C_3 and Al and the lattice strain developed within the matrix as a function of laser parameters. From Table II it may be noted that WC content in the alloyed zone decreases and W_2C content increases with increase in applied power (at a scan speed of 0.012 m/s) while, the mass fraction of other carbides do not vary significantly. The decreased mass fraction of WC content with increase in applied power is attributed to increased dissolution with increase in applied power. On the other hand, with increase in scan speed (at an applied power of 3.5 kW) WC content increases significantly due to less dissolution. However, at a very high scan speed WC content in the alloyed zone decreases marginally possibly due to less mass fraction of WC supplied during coating due to

a very low interaction time. From the marginal variation of other carbides and the irregular trend observed on the variation of carbides with laser parameters it may be concluded that immediately during laser surface alloying process there is dissolution of WC and formation of other carbides and the tendency of different carbides formation is governed by the free energy change associated with carbide formation. On the other hand, Al_4C_3 content remains almost same and does not vary with process parameters. The free energy change associated with the formation of different carbides follow the following equations [19,20]:

$4Al + 3C = Al_4C_3$

$\Delta G_{933\ K}$ = -58.89 kJ/mol

$W + C = WC$

$\Delta G_{1150\ K}$ = -36.57 kJ/mol

$W + WC = W_2C$

$\Delta G_{1575\ K}$ = -34.18 kJ/mol

$23\ Cr + 6C = Cr_{23}C_6$

$\Delta G_{1150\ K}$ = -68.35 kJ/mol

From the free energy of formation of different carbides it may be noted that the free energy of formation associated with aluminium carbide (Al_4C_3) formation is minimum. Hence, the probability of formation of Al_4C_3 is maximum following dissolution of WC. During laser processing WC may dissolve by the following mechanism: (a) prior to alloying by heating effect during powder feeding, (b) while intermixing with the liquid aluminium during alloying. However, due to a much lower melting temperature of Al as compared to WC, the probability of mechanism (a) is maximum for WC dissolution. Hence, it may be concluded that laser parameters play a crucial role in determining the degree of dissolution of WC

particles. As soon as there is alloying of aluminium with dissociated WC, Al_4C_3 phase formation occurs. Then the other carbide formation proceeds.

3.3 Microhardness Measurement

Figure 10 shows the microhardness profile with the depth from the surface of (a) as-received and laser composite surfaced Al lased under different process parameters. From Figure 10, it is evident that the microhardness of the alloyed zone is significantly improved to as high as 200-650 VHN as compared to 22 VHN of as-received substrate. The orders of magnitude enhanced microhardness at the top surface as compared to as-received alloy is attributed to the presence of carbides (both unmelted and resolidified one) and refinement of microstructure. Furthermore, the microhardness is maximum at the top surface and decreases with the depth from the surface. The decrease in microhardness with depth is possibly due to coarsening of microstructure with depth and also presence of a large volume fraction of carbides at the surface, which decreases with depth. The maximum improvement in hardness achieved when lased at an applied power of 3.5 kW and scan speed of 0.03 m/s. Laser parameters play a role in determining the microhardness at the surface and its distribution with depth. Increase in applied power from 3 kW to 3.5 kW (at a scan speed of 0.012 m/s) was found to decrease the average surface microhardness from 390 to 200 VHN. The decrease in microhardness with increase in applied power is attributed to increased depth of melting at a higher power and hence a lower volume fraction of WC (when the same scan speed is applied). On the other hand, decrease in scan speed from 0.04 to 0.03 m/s (at an applied power of 3.5 kW) was found to increase the microhardness from 425 to 650 VHN. The increase in microhardness with decrease in scan speed is due to a high interaction time at a low scan speed and hence, more powder delivered during surface alloying, leading to an increased volume fraction of precipitates.

In this regard, it is relevant to mention that in the past, several attempts have been made to disperse carbide particles on the surface of aluminium based alloy by laser surface alloying technique. Table III summarizes the ported literatures on development of carbide dispersed surface on aluminium based alloy by laser surface alloying technique. Reaction synthesis of WC+TiC and intermetallics of Al and Ni was successfully attempted on Al6061 alloy by feeding (Ti+C+W) + Ni+Al (and Al_2O_3) using Nd:YAG laser as a heat source for ignition and propagation [21]. The significant enhancement in hardness was reported (with a maximum of 1100 VHN) as compared to as-received substrate. The improved hardness was attributed to the presence of fine carbides and intermetallics in aluminium matrix [21]. Application of Ti+SiC as feedstock in laser surface alloying led to development of highly refined (of particle size less than 3 μm) TiC particles dispersion in the matrix consisting of Si, Ti_3Al and $TiAl_3$ with improved microhardness to 650 VHN as compared to as-received substrate [22]. Proper selection of laser parameters is also capable of controlling the distribution of particles and its volume fraction. Development of graded SiC dispersed aluminium matrix composite was reported by Dutta Majumdar et al [4] with a maximum improvement of hardness to a value of 250 VHN. In all the cases, it was observed that the mechanism of hardening is mainly dispersion hardening and hence, area fraction of particles play the main role in determining the microhardness of the alloyed zone. In the present study, laser surface alloying of Al with WC+Co+NiCr increases the microhardness significantly due to dispersion of WC and resolidified carbides in the matrix and area fraction of particles and its distribution are controlled by laser power. The improvement in microhardness is attributed to distribution of carbides. The improved hardness by laser surface alloying is beneficial for improving wear resistance properties.

3.4 Wear Analysis

Figure 11 compares the kinetics of fretting wear (against tungtsten carbide surface) in terms of cumulative depth of wear with time for as-received (plot 1 and plot 2) and laser surface alloyed aluminium (plot 3 and plot 4) against WC ball measured by friction and wear monitor (Model: DUCOM, TR-283M-M4) at applied load of 0.5 kg (plot 2 and plot 4) and 1 kg (plot 1 and plot 3) for a period of 1800 s at an oscillating frequency 10 s^{-1}. From Figure 11, it may be noted that the wear rate of both as-received and surface alloyed samples increases with increase in applied load (from 0.5 kg to 1 kg). Furthermore, in as-received aluminium, the wear rate is very high at the initial period following which it decreases. The initial increased rate of wear in as-received aluminium is due to a combined action of abrasion and fretting. The wear rate decreases at a later stage due to the accumulation of worn out debris at the interface between the mating surfaces and hence, reducing the aggressiveness of the abrasion. On the other hand, in laser surface alloying sample, the wear rate is very low and remains constant all throughout. The significantly lower rate of wear in laser surface alloyed sample as compared to as-received one is due to an increased hardness of the surface. The kinetics of wear is laser composite surfaced component was found to depend on the size, shape and distribution of particles and interfacial strength between the particle and matrix. Dispersion of SiC in Al was found to improve the wear resistance by hardening of the surface and reduction of coefficient of friction [23]. Laser surface cladding of WC+Mo on Al6061 alloy was found to improve the wear resistance significantly due to the presence of tough Mo and hard WC and good interfacial bonding between WC and Al matrix [24]. Improvement in wear resistance was also noticed in WC dispersed aluminium matrix composite surface developed by laser surface alloying technique [21]. Detailed study of coefficient of friction of as received and laser surface alloyed samples were undertaken to understand the mechanism of wear in details. Figure 12 summarizes the coefficient of friction of as-received vis-à-vis

laser surface alloyed aluminium against WC surface at varied load under fretting wear. From Figure 12, it is relevant to mention that in as-received aluminium, the coefficient of friction remains constant during wear study and decreases (from 0.18 to 0.10) with increase in load. The decrease in coefficient of friction with increase in load is attributed to the formation of more worn out debris when a high load is applied and subsequently, changing the wear mode from two body to three body wear where, worn aluminium debris act as lubricant and hence, reduces the coefficient of friction. Furthermore, the coefficient of friction of as-received aluminium is significantly lower than laser surface alloyed aluminium. The increased coefficient of friction in laser surface alloyed aluminium is attributed to roughening of the surface due to removal of aluminium from the metal matrix composite during wear and presence of only carbides in the microstructure. Table II summarizes the coefficient of friction of as-received vis-à-vis laser surface alloyed aluminium against WC surface as a function of applied load. The marginal reduction in coefficient of friction with increase in applied load may be noted. Table III summarizes the mechanical properties (microhardness and wear resistance) of laser surface alloyed and clad Al with carbide particles developed by laser processing. From Table III it may be noted that microhardness enhancement varied from 250 to 1100 VHN based on the nature of carbide particles and its distribution. In this regard, a maximum improvement in wear resistance (almost two orders on magnitude as compared to substrate) is achieved when cladding of WC was carried out on AA6061 Al alloy [24]. Enhancement of coefficient of friction in laser surface alloyed aluminium based alloy (Al-356) with 96% WC + 2%Ti+2% Mg was also reported by Staia *et al*. [25]. In contrast, a decrease in coefficient of friction was noticed in SiC dispersed Al surface developed by laser surface alloying routes [4]. Addition of Ti and C along with WC was reported to enhance the hardness to as high as 1100 VHN as compared to as-received substrate [21].

Figure 13(a,b) shows the scanning electron micrograph of worn out surface of (a) as-received aluminium and the (b) same at high magnification against WC ball at an applied load of 1 kg. From Figure 13(a), it may be noted that there is presence of excessive deformation in the worn scar with the presence of damage from the sub-surface region. The microstructure at high magnification shows the presence of worn out debris (1) and micro-grooves (2). From Figure 13, it may be concluded that the mechanism of wear in as-received aluminium at an applied load of 1 kg is predominantly the combination of high stress abrasion and fretting in nature. Presence of excess worn out debris acts as barrier while wear and hence, reduces the coefficient of friction in course of wear. Figure 14(a-b) show the scanning electron micrograph of worn out surface of (a) laser surface alloyed aluminium and the same (b) at high magnification against WC ball at an applied load of 1 kg. A comparison of Figure 14(a) with Figure 13(a) shows that the track dimension of worn out surface is significantly lower as compared to as-received aluminium. A significant low dimension of laser surface alloyed scar is attributed to a lower material removal due to wear in laser alloyed surface as compared to as-received aluminium due to the high hardness of the surface alloyed aluminium. The same at high magnification shows that the presence of very fine scratch marks (1), microcracks (2), deformation bands (3) and fragmented carbides (4). The deformation band was observed due to the deformation of matrix. The presence of fragmented carbides is responsible for increasing the coefficient of friction during wear. Hence it may be concluded that the mechanism of wear is mainly because of removal of aluminium by abrasive action, deformation of matrix due to excessive load and excessive damage by fretting action.

4. Summary and Conclusions

In the present study laser surface alloying of aluminium with WC+Co+NiCr (in the ratio 70:15:15) has been successfully achieved. From the detailed investigations, the following conclusions may be drawn:

1. Laser parameters play a crucial role in determining the microstructures and surface topography of the alloyed zone. Defect free microstructures are developed only under optimum laser parameters.
2. The microstructure of the alloyed zone formed under optimum processing regime consists of a defect free and homogeneous alloyed zone with the dispersion of WC, W_2C, Al_4C_3, Al_9Co_2, Al_3Ni, $Cr_{23}C_6$, and Co_6W_6C in grain refined aluminium matrix. The phases formed were confirmed by XRD and EBSD analysis.
3. Morphology of the alloyed zone is columnar at the near interface region which changes to dendritic and equiaxed towards the surface.
4. The microhardness of the alloyed zone is significantly increased (200 VHN to 650 VHN) as compared to 22 VHN of as-received substrate. A graded decrease in microhardness from surface to substrate was observed which is attributed to the change in the carbide content and grain size with depth.
5. The kinetics of fretting wear against WC ball was significantly decreased in laser surface alloyed sample as compared to as-received aluminium. The improvement in wear resistance was attributed to the presence of carbides in grain refined aluminium.
6. The coefficient of friction of laser alloyed aluminium was significantly higher than that of as-received aluminium.

References

[1] C. Grard, Aluminum and Its Alloys, Their Properties, Thermal Treatment and Industrial Application, D. Van Nostrand Co., New York, 1922.

[2] K. G. Budinski, Surface Engineering for Wear Resistance, Prentice Hall, New Jersey, 1988

[3] J. Dutta Majumdar, I. Manna, International Materials Review, 56 (2011) 341-388.

[4] J. Dutta Majumdar, B.R. Chandra, A.K. Nath, I. Manna, Mater. Sci. Eng. A 433 (2006) 241–250

[5] J. Dutta Majumdar, B. Ramesh Chandra, R. Galun, B.L. Mordike, I. Manna, Comp. Sci. Technol. 63 (2003) 771–778.

[6] J.Dutta Majumdar, B. Ramesh Chandra, B.L. Mordike , R. Galun , I. Manna, Surf. Coat. Technol. 179 (2004) 297–305.

[7] D. Pantelis, A. Houndri, Y. Chryssoulakis, J. Phys. IV 1 (1991) 111–116.

[8] D.K. Das, K.S. Prasad, A.G. Paradkar, Mater. Sci. Eng. A 174 (1994) 75–84

[9] W.J. Tomlinson, A.S. Bransden, J. Mater. Sci. Lett. 13 (1994) 1086–1088.

[10] J.L. de Mol Van Otterlo, J.Th.M. De Hosson, Proc. Comp. Meth. Exp. Meas. Surf. Treat. Effect 1 (1995) 255–263

[11] L. Dubourg, H. Pelletier, D. Vaissiere, F. Hlawka, A. Cornet, Wear 253 (2002) 1077–1085

[12] Y.Y. Qiu, A. Almeida, R. Vilar, J. Mater. Sci. 33 (1998) 2639–2651.

[13] Y.Y. Qiu, A. Almeida, R. Vilar, Scrip. Metal. Mater. 33 (1995) 863–870.

[14] Y.T. Pei, J.Th.M. De Hosson, Acta Mater. 48 (2000) 2617–2624

[15] J.M. Pelletier, P. Sallamand, B. Criqui, J. Phys. 4 (1994) 93–96.

[16] P. K. Rohatgi, Defence Science Journal, 43 (1993) 323-349.

[17] M.G. Fontana (Ed.3), Corrosion Engineering, McGraw-Hill, New York, 1987, p. 71.

[18] B. D. Cullity, (1956). Elements of X- ray diffraction, Addison-Wesley.

[19] R. G. Coltters, Mater. Sci. Eng. 76 (1985) 1-50

[20] D. K. Gupta, L.L. Seigle, Metall. Trans. A. 6 (1975) 1939-1944

[21] H.C. Man, Y.Q. Yang, W.B. Lee, Surf. Coat. Technol. 185 (2004) 74– 80

[22] H.C. Man, S. Zhang, F.T. Cheng, T.M. Yue, Scripta Mater. 46 (2002) 229–234

[23] J. Dutta Majumdar, B. Ramesh Chandra, I. Manna, Wear 262 (2007) 641-648.

[24] P.H. Chong, H.C. Man, T.M Yue, Surf. Coat. Technol. 145 (2001) 51-59

[25] M.H. Staia, M. Cruz, N.B. Dahotre, Wear 251 (2001) 1459–1468.

Figure 1 (a) Scanning electron micrograph, and (b) X-ray diffraction profile of the precursor powder mixture (70WC+15Co+15NiCr) used in the present study.

Figure 2 Scanning electron micrographs of cross-section of laser composite surfaced aluminium using a laser power of 3.5 kW and scan speed of (a) 0.04 m/s and (b) 0.012 m/s.

Figure 3 Scanning electron micrographs of the top surface of laser alloyed aluminium with WC+Co+NiCr lased with a power of (a) 3 kW, (b) 3.5 kW and scan speed of 0.012 m/s.

Figure 4 Scanning electron micrographs of cross-section of (a) laser alloyed zone and (b) near surface region, (c) intermediate region, and (d) near interface region.

Figure 5 Scanning electron micrograph of the cross section of laser surface alloyed aluminium with WC+Co+NiCr showing different types of precipitate.

Figure 6 Scanning electron micrograph of the alloyed zone showing the interface between globular precipitate and the matrix.

Figure 7 Scanning electron micrograph of the interface between the alloyed zone and substrate.

Figure 8 High resolution transmission electron micrographs of laser surface alloyed aluminium showing (a) matrix and (b) precipitates.

Figure 9 X-ray diffraction profiles of the top surface of laser surface alloyed Aluminium showing the effect of (a) applied power and (b) scan speed on the phase formation behaviour.

Figure 10 Variation of microhardness with depth for different processing condition.

Figure 11 Variation of cumulative depth of wear with time for as received (plot 1 and plot 2) and laser surface alloyed aluminium lased with an applied power of 3.5 kW and scan speed of 0.03 m/s (plot 3 and plot 4) worn against WC ball at an applied load of 0.5 kg (plot 2 and plot 4) and 1 kg (plot 1 and plot 3).

Figure 12 Variation of Coefficient of Friction with time for as received (plot 1 and plot 2) and laser surface alloyed aluminium lased with an applied power of 3.5 kW and scan speed of 0.03 m/s (plot 3 and plot 4) worn against WC ball at applied load of 0.5 kg (plot 2 and plot 4) and 1 kg (plot 1 and plot 3).

Figure 13 Scanning electron micrographs of worn out surface of (a) aluminium and the (b) same at high magnification followed by wear against WC ball at applied load of 1 kg and 1800 s of wearing.

Figure 14 Scanning electron micrographs of worn out surface of (a) laser surface alloyed aluminium and the (b) same at high magnification followed by wear against WC ball at an applied load of 1 kg and 1800 s of wearing.

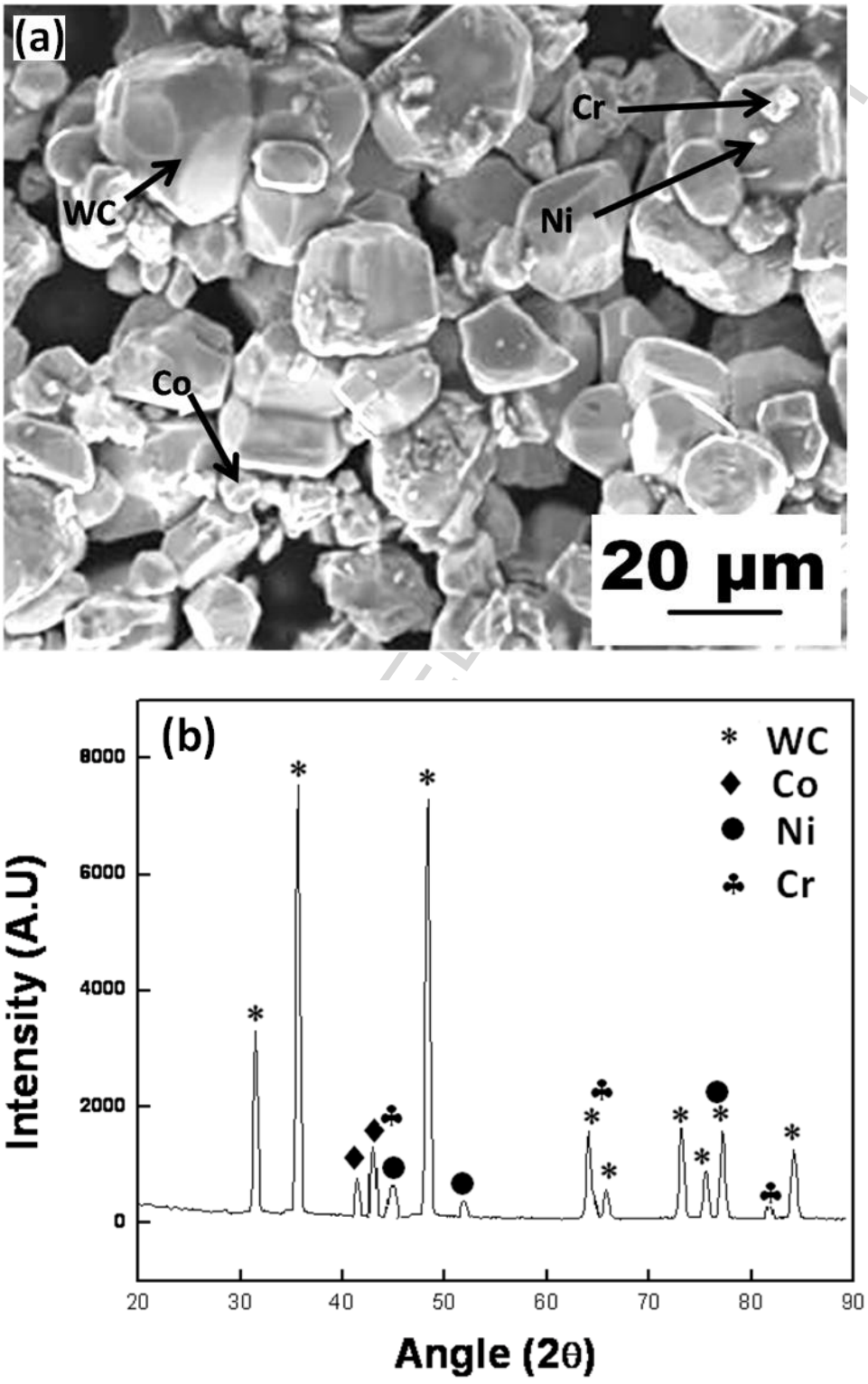

Fig. 1

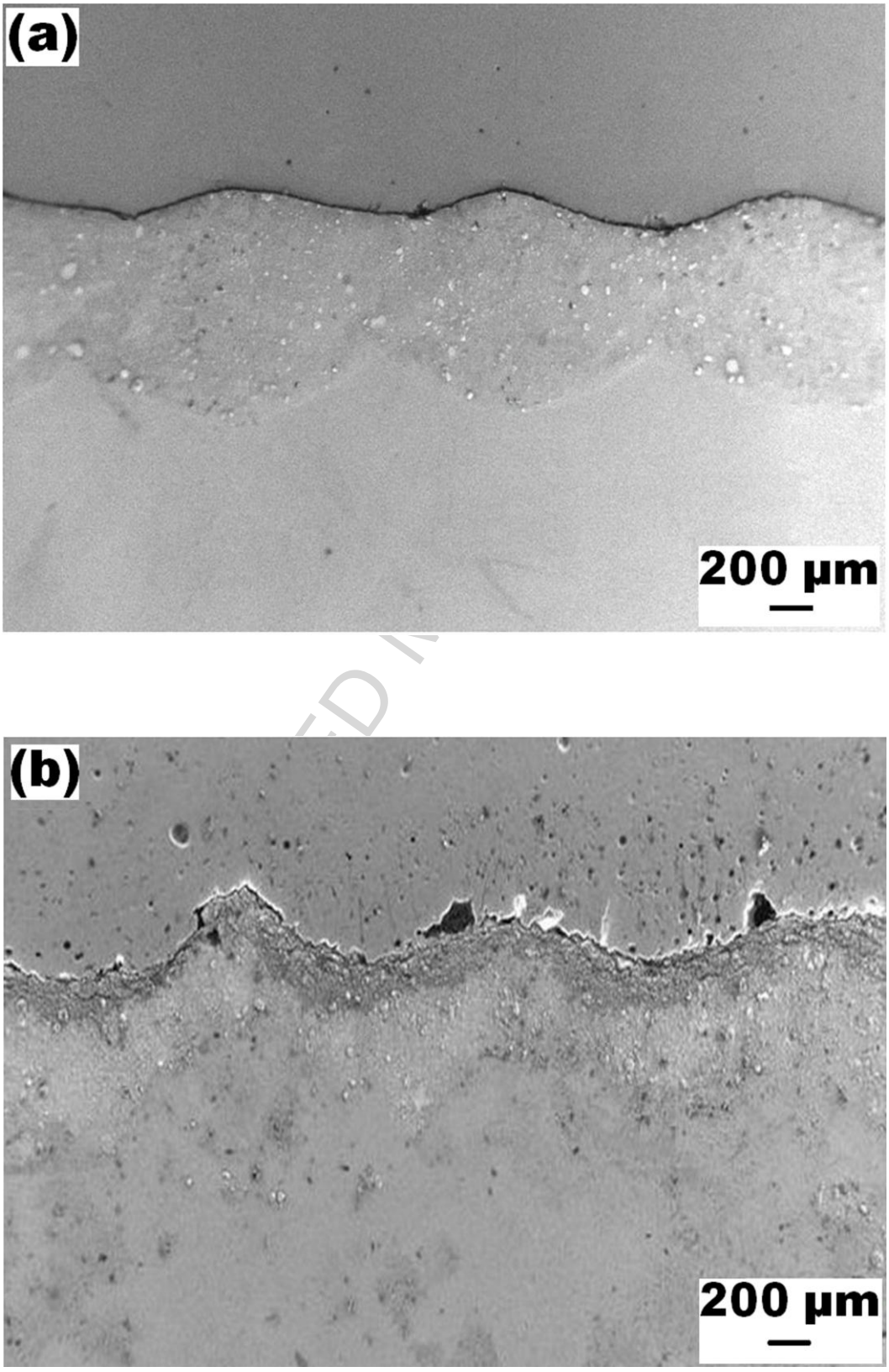

Fig. 2

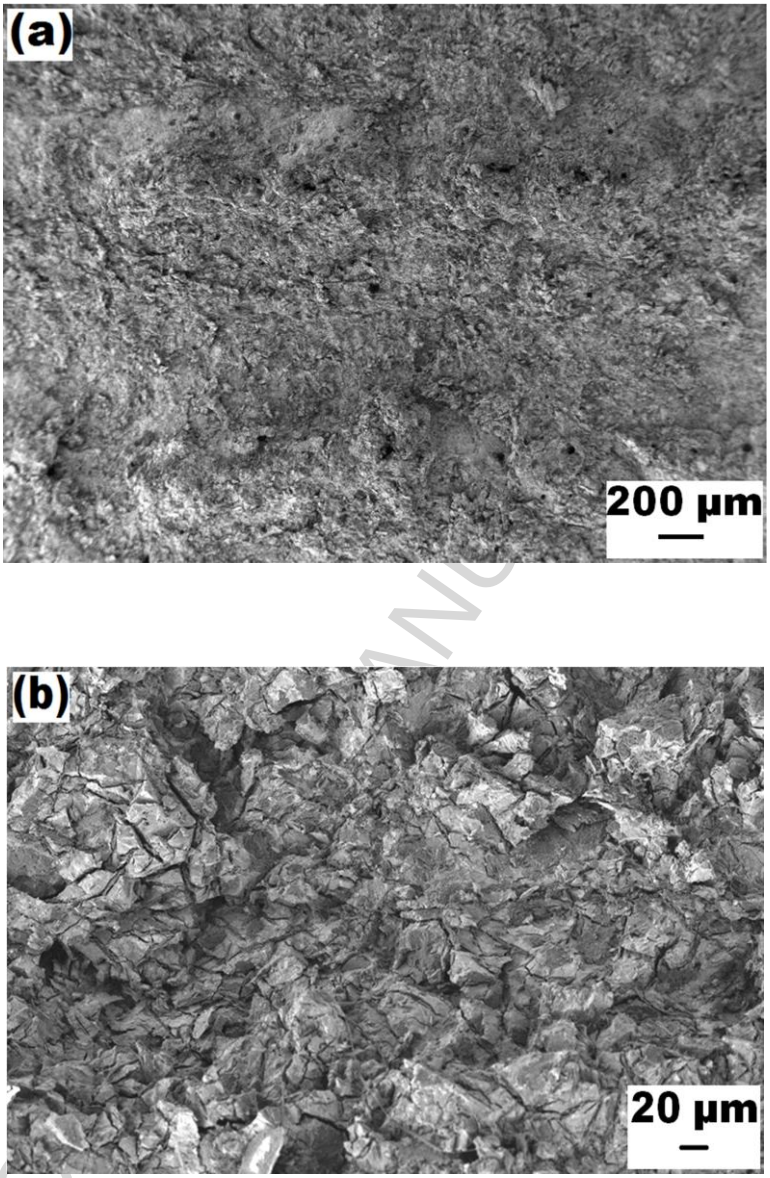

Fig. 3

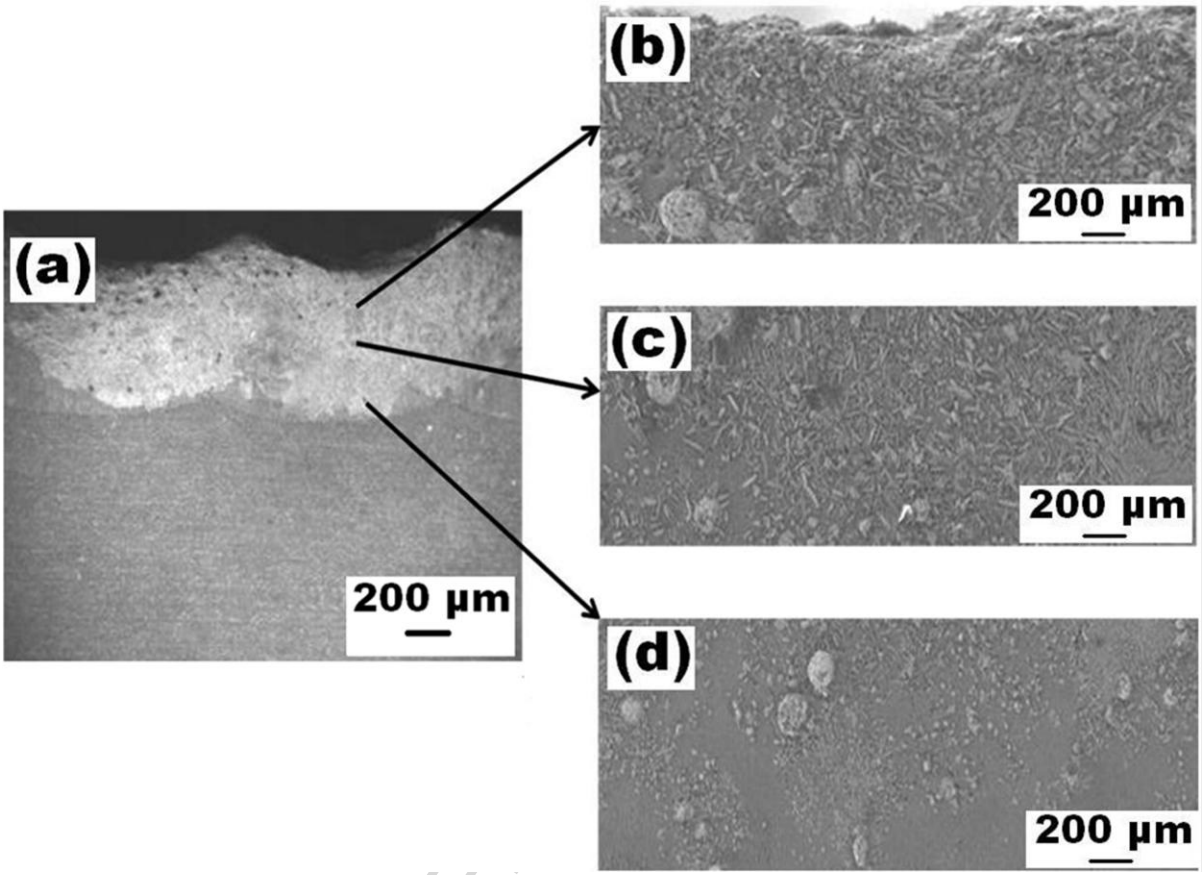

Fig. 4

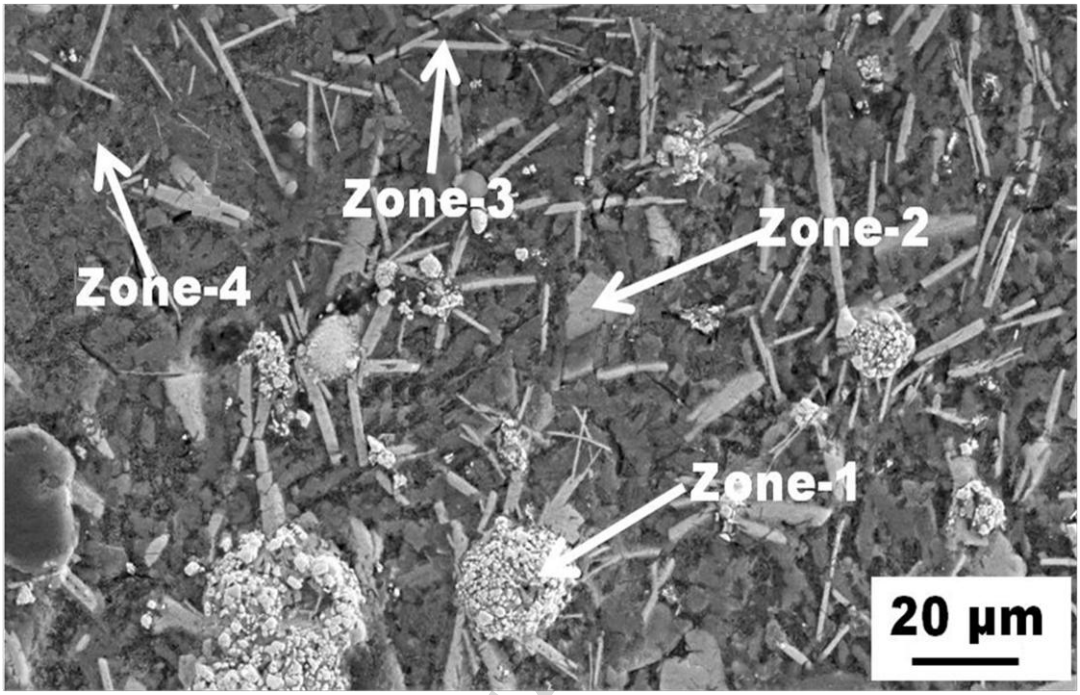

Fig. 5

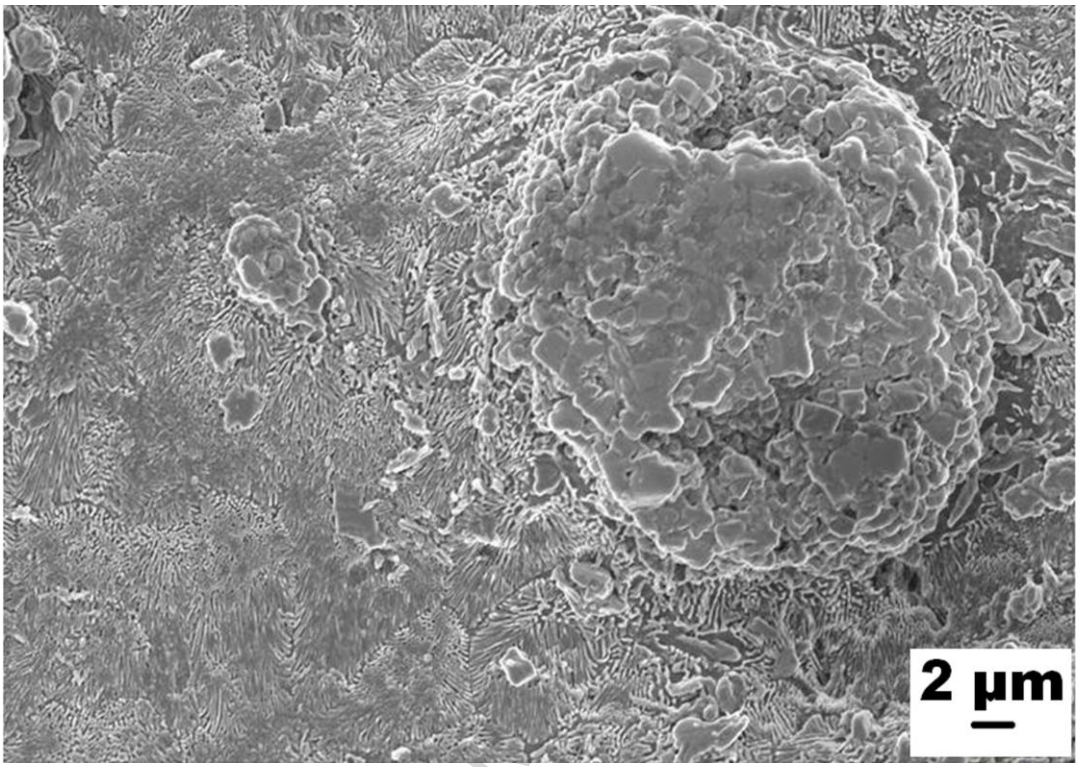

Fig. 6

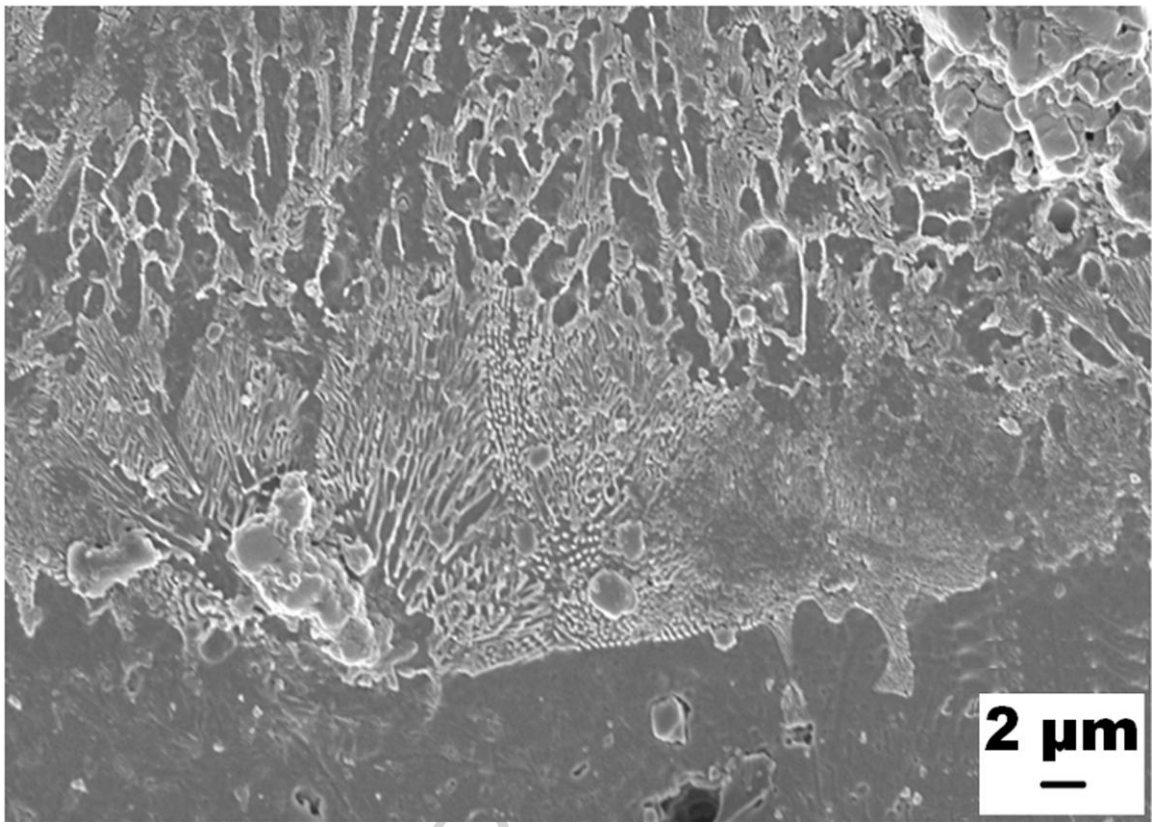

Fig. 7

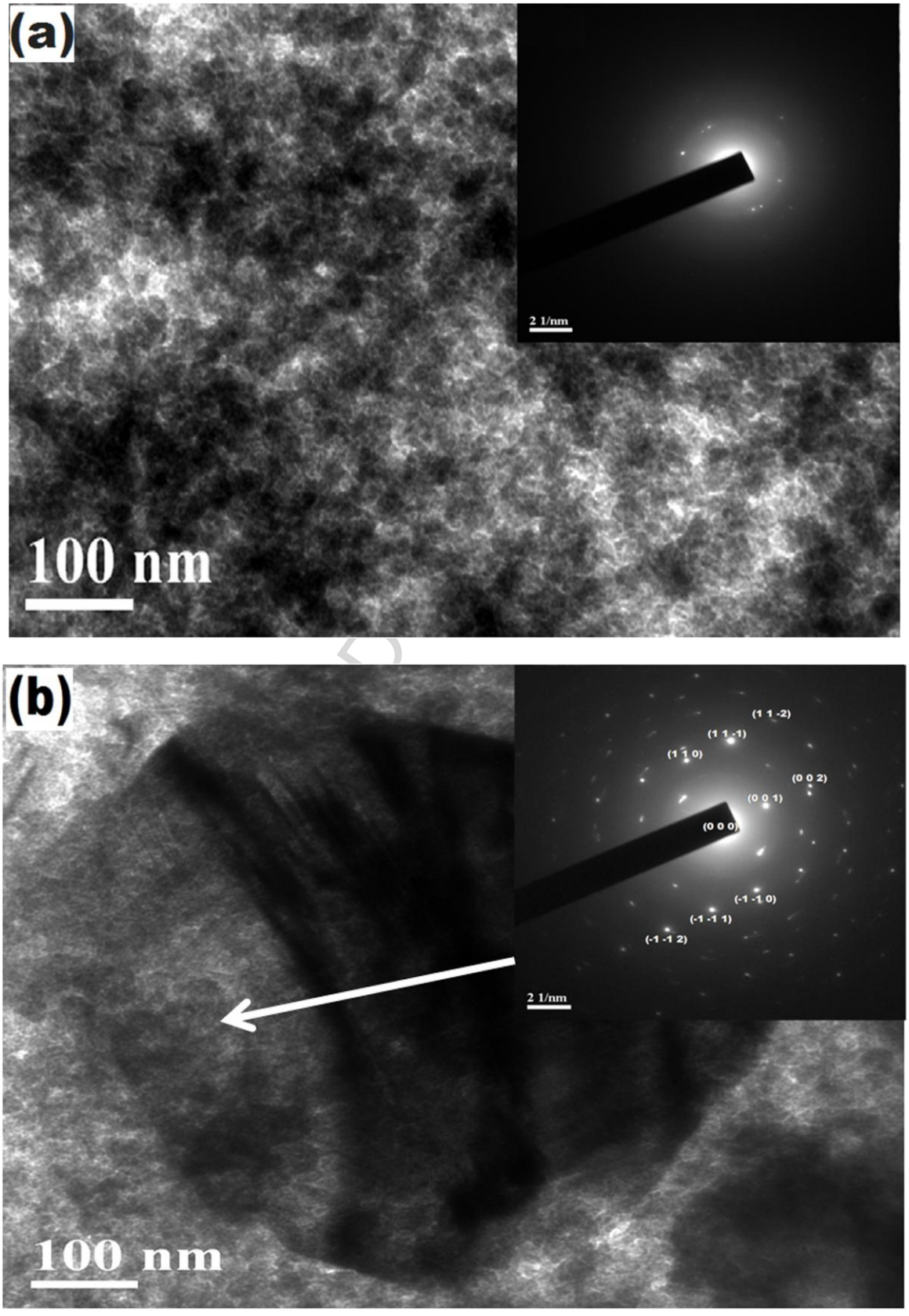

Fig. 8

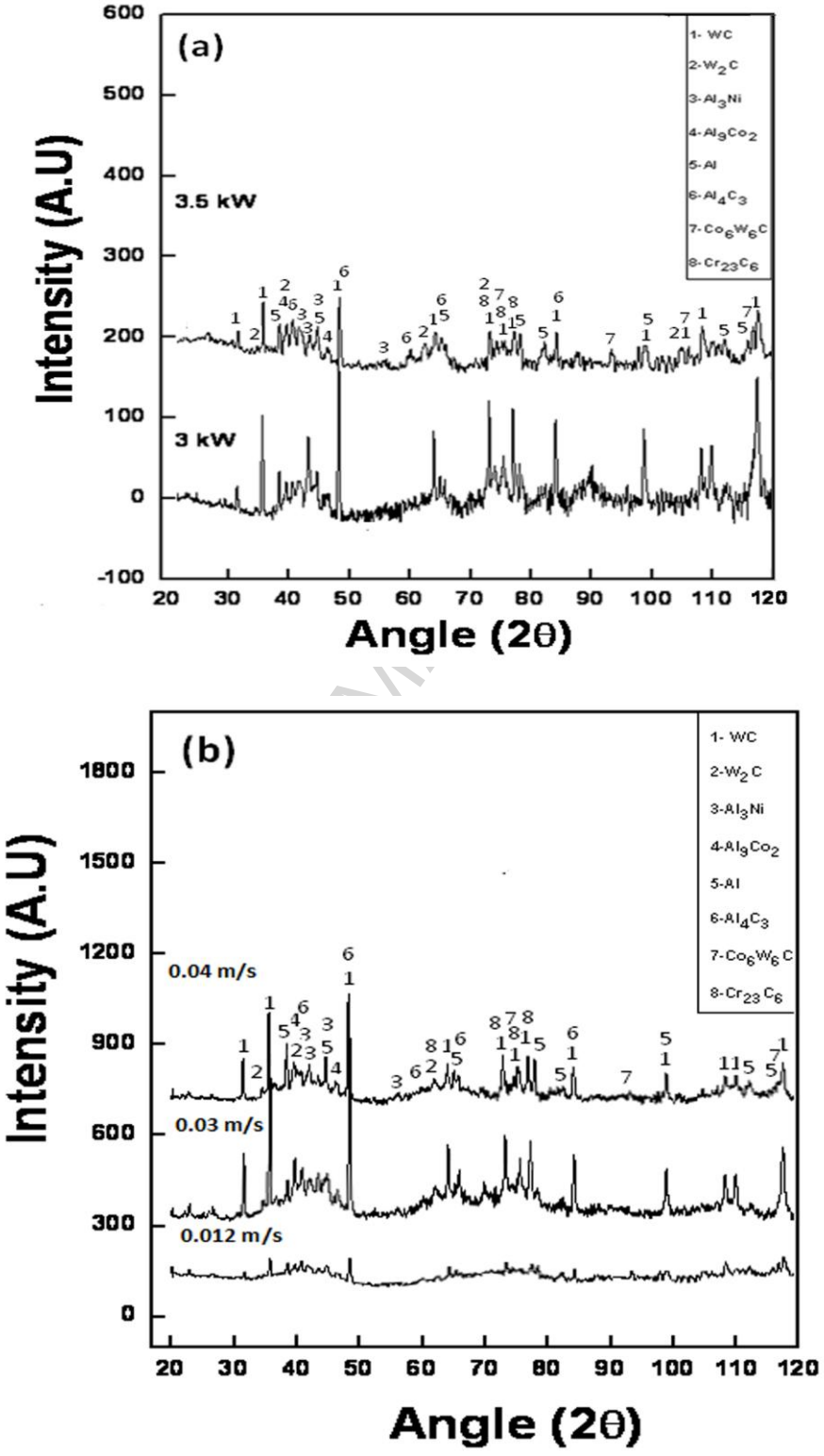

Fig. 9

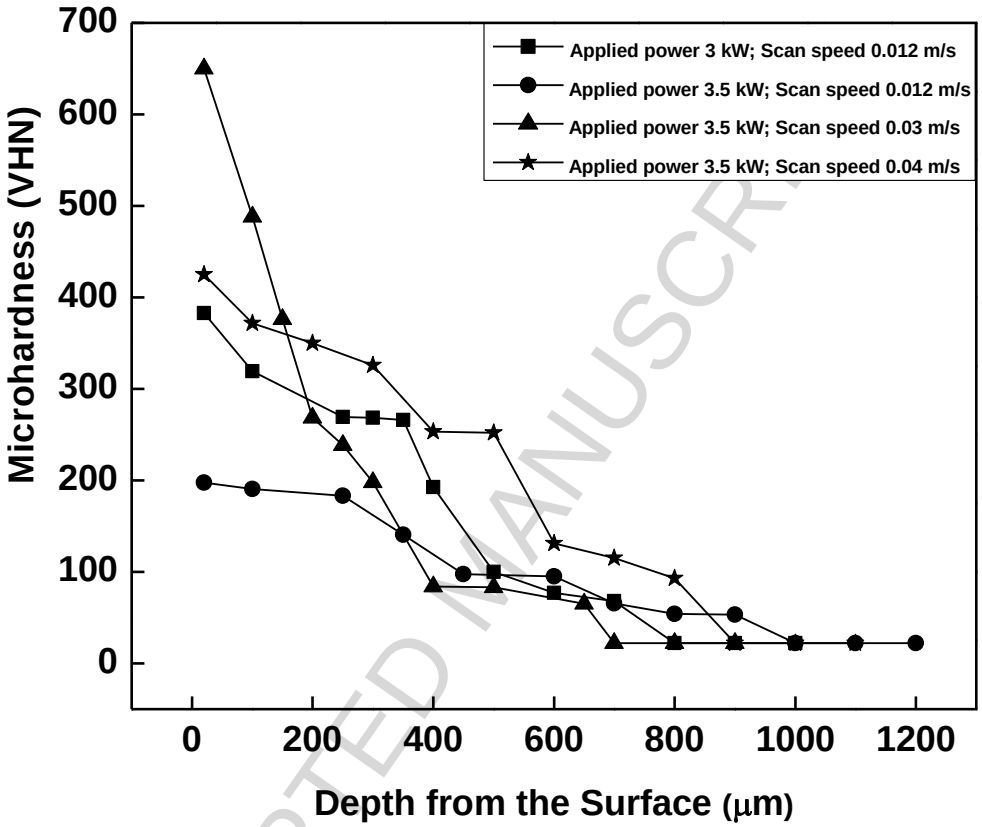

Fig. 10

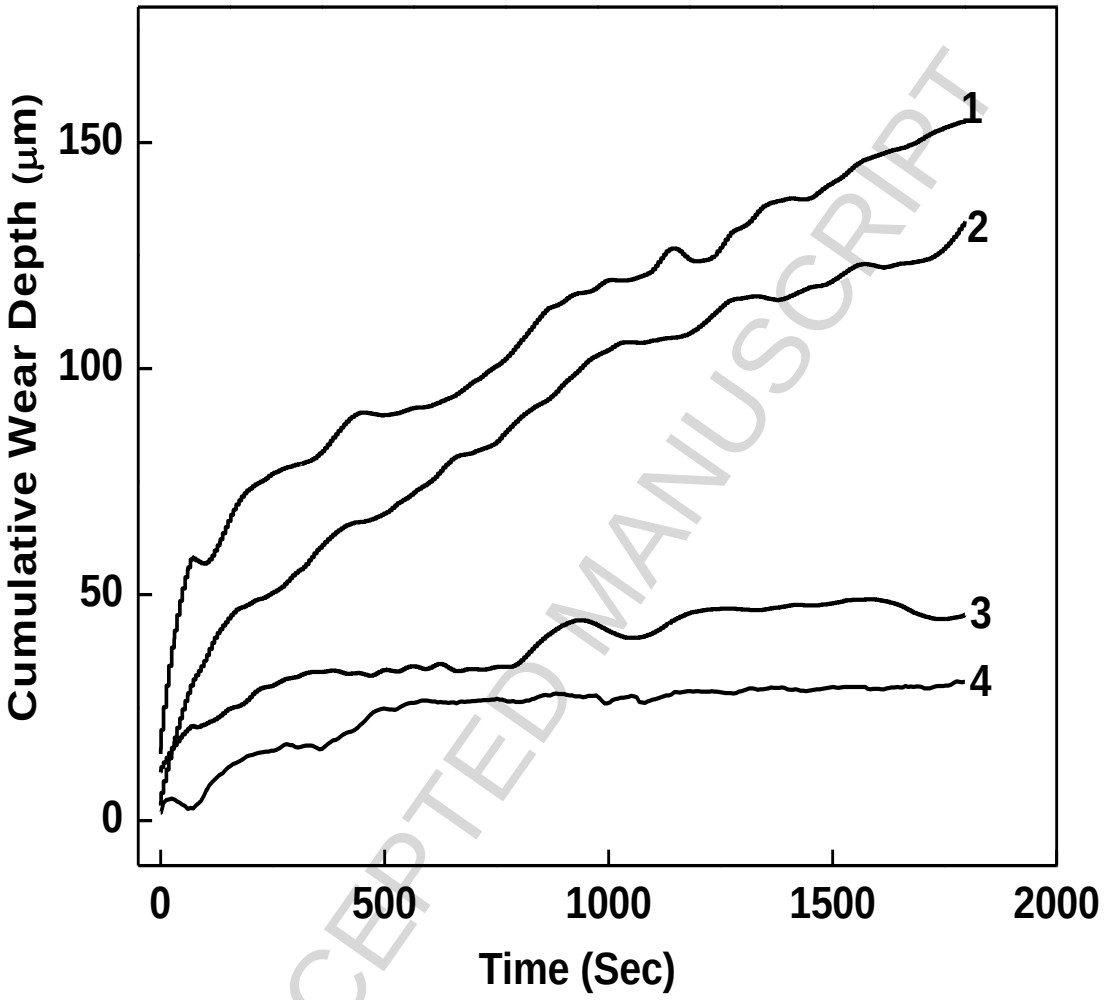

Fig. 11

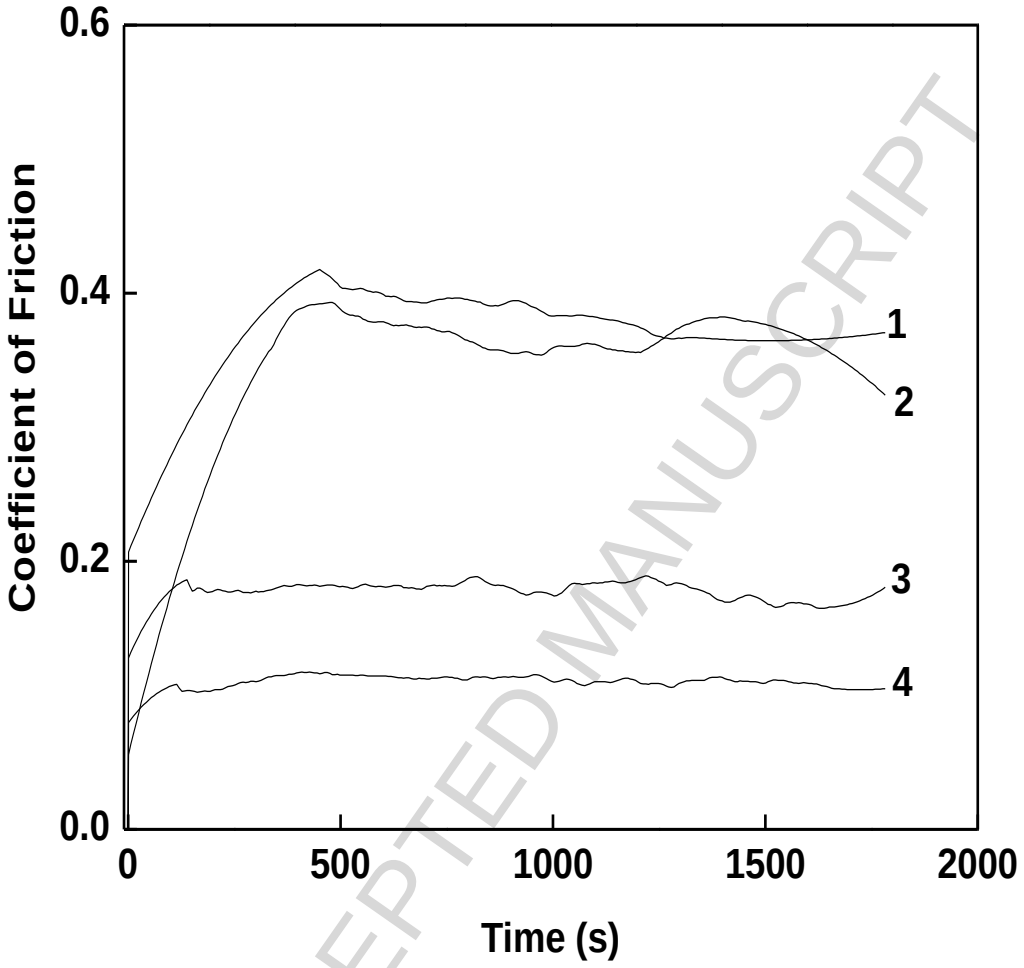

Fig. 12

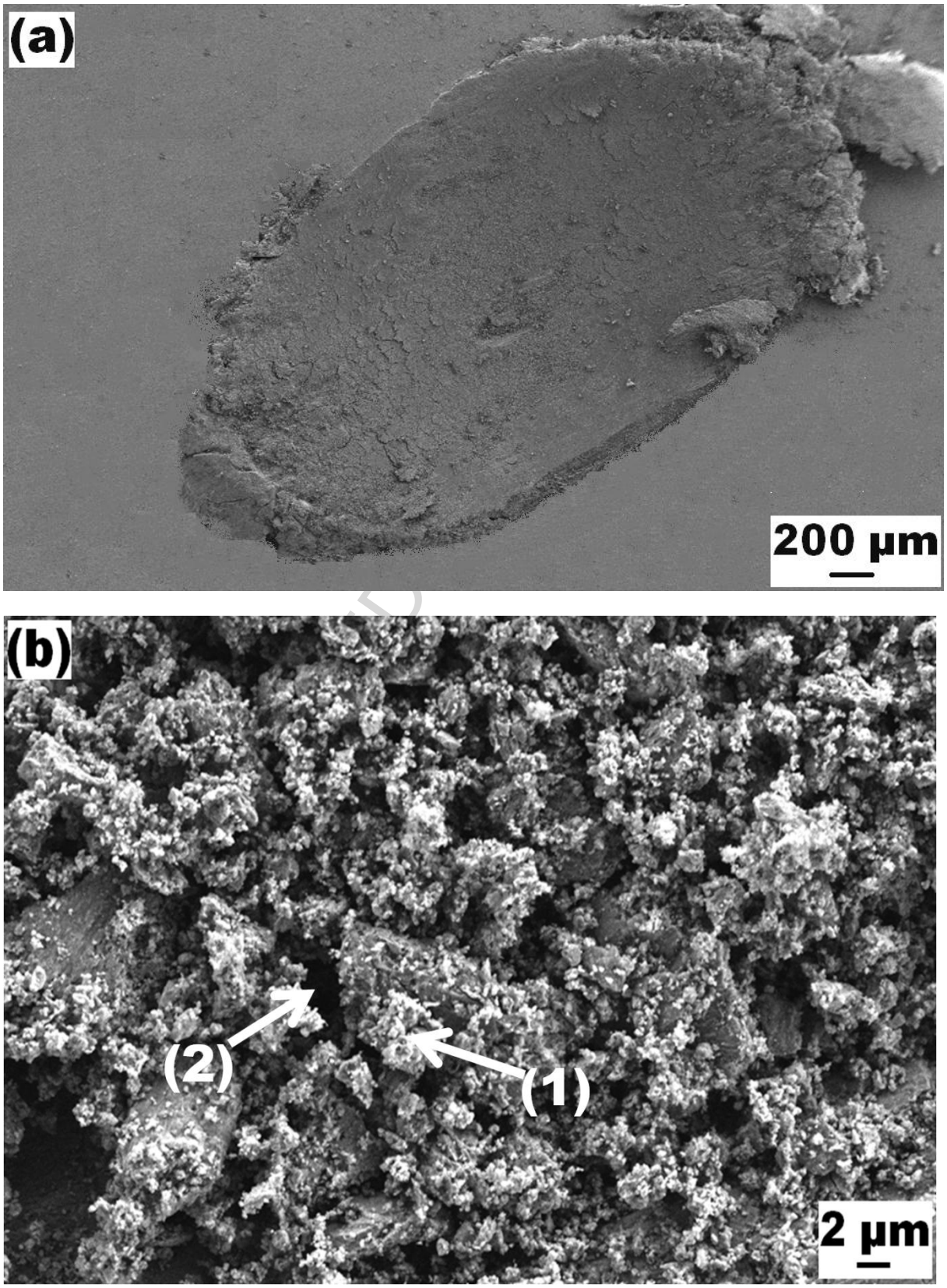

Fig. 13

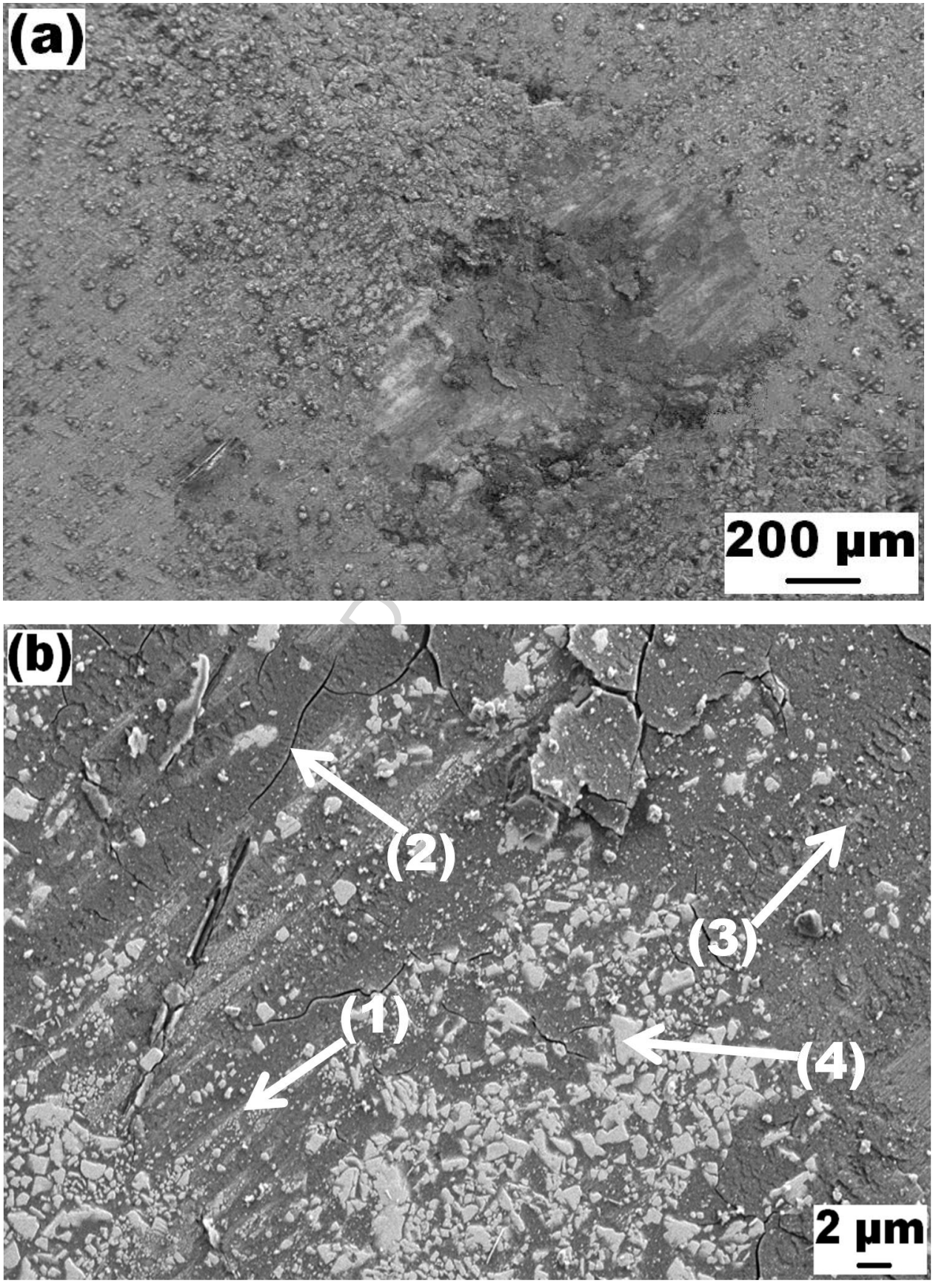

Fig. 14

Table I: Composition analysis of different zones of laser alloyed cross-section as shown in Figure 4

Elements	Composition in weight%			
	Zone-1	Zone-2	Zone-3	Zone-4
Al	0.00	11.49	39.34	80.48
W	100	88.51	54.83	2.60
Co	0.00	0.00	1.24	6.38
Ni	0.00	0.00	1.57	9.72
Cr	0.00	0.00	3.02	0.81

Table II: Variation of mass fraction and lattice strain with laser parameters

Laser Power (kW)	Scan Speed (m/s)	Mass fraction of different phases present in the alloyed zone (%)								Lattice Strain in Al (%)
		WC	W_2C	Al	Al_4C_3	Al_3Ni	Al_9Co_2	$Cr_{23}C_6$	Co_6W_6C	
3	0.012	40.99	5.87	8.8	16	1.6	6.47	9.33	10.91	0.170
3.5	0.012	37.99	9.35	11.04	15.81	6.98	2.62	7.97	8.22	0.363
3.5	0.03	47.22	7.12	7.78	15.13	2.65	5.98	7.48	6.63	0.116
3.5	0.04	41.32	6.59	16.8	13.58	4.75	4.66	6.67	5.54	0.116

Table III Summary of Mechanical Properties in Carbide Dispersed Aluminium Developed by Laser Surface Alloying Process

Sl. No	Substrate	Laser used	Precursor powder	Hardness	Wear	Reference
1	Al-Mg alloy (A5083)	CO_2 laser	TiC-Cu composite powders (Cu-10, 20, 30, 50 and 60 mass %)	MMC layer -500 VHN. Al-Mg alloy substrate- 100 VHN	Wear resistance increased up to six times to that of Al-Mg alloy substrate. (abrasive wear test)	[23]
2	AA6061 aluminum alloy	Nd-YAG laser	Mo and WC (wt% of WC- 20, 40, 60, 80, 100)	Clad layer- 766 VHN (For 100 % WC)	Wear resistance increased to almost two orders of magnitude as compared to the Al-Mg alloy substrate.	[22]
3	Al-356 alloy	Nd-YAG laser	Powders with 96 wt.% WC, 2 wt.% Ti and 2 wt.% Mg	Alloyed zone- 590.75 VHN (Scan speed-300 cm/min). As-received alloy substrate- 80 VHN	Coefficient of friction is 0.78 on laser clad surface as compared to 0.5 in substrate	[24]
4	Al 6061 alloy	Nd:YAG laser	Ti+WC+C, Ti+W+C, Ni-Al and Ni-Al2O3 powders	Clad Layer- 800 to 1100 VHN as compared to 80 VHN of substrate	Wear resistance increased	[19]
5	CP Al	CO_2 laser	SiC and Al + SiC (at a ratio of 1:1)	Alloyed zone- 250, As-received substrate- 25 VHN.	Wear resistance is doubled	[4]
6	AA6061 Al alloy	Nd-YAG laser	60 wt%Ti + 40 wt% SiC powders	MMC layer- 650 VHN, As-received alloy substrate- 75 VHN	Not Available	[20]
7	CP Al	Nd-YAG laser	WC+Co+NiCr (in the ratio of 70:15:15)	Improved hardness to 650 VHN as compared to 22 VHN of CP Al	Improvement in wear resistance to 4 times as compared to as-received substrate	The present study

Research Highlights

- Optimization of process parameters for the development of defect free microstructure.
- Detailed mechanism of microstructural evolution under laser processing conditions.
- To understand the role of process parameters on the distribution of carbides.
- Improved hardness of the alloyed zone (650 VHN) as compared to substrate (22 VHN).
- Improved wear resistance (4 times as compared to substrate) of the alloyed zone.